Advances in Concrete Construction, *Vol. 17, No. 1 (2024) 45-52*
https://doi.org/10.12989/acc.2024.17.1.045

Performance of paraffin mixed concrete subjected to combined freeze-thaw and chloride environment

Hiroshi Maruta [a], Dhruva Narayana Katpady*, Hirotaka Hazehara [b] and Masashi Soeda [c]

Department of Civil Engineering, Fukuoka University, Jonan ku, Nanakuma 8-19-1, Fukuoka 814-0180, Japan

(*Received August 25, 2023, Revised May 31, 2024, Accepted June 24, 2024*)

Abstract. In this study, the fresh properties of paraffin-mixed concrete, compressive strength, resistance to frost damage, and resistance to composite deterioration under freeze-thaw and salt environment were investigated. The compressive strength of paraffin-mixed concrete was almost the same as that of unmixed concrete, and no decrease in strength was observed, unlike the concrete with entrained air in consideration of freeze-thaw resistance. Concerning the freeze-thaw resistance of paraffin-mixed concrete, the relative dynamic modulus of elasticity (RDME) did not decrease even without entrained air. In addition, no decrease in the RDME was observed in the combined deterioration with salt damage, and it was confirmed that the mass reduction was suppressed compared to the concrete without paraffin. The freeze-thaw resistance of concrete when paraffin is mixed may be improved due to the reduction in the amount of frozen water and the mixed paraffin particles exist in the concrete as pore fillers with a size of 200 μm or less, which act as substitutes for air voids. This resulted in reduction of the apparent air void spacing and thereby relieving the pore pressure.

Keywords: dynamic modulus; freeze-thaw; paraffin; pore structure; salt damage; scaling

1. Introduction

Concrete structures in cold regions suffer from freeze-thaw damage such as cracks, pop-outs, and scaling due to the deleterious expansion of water contained in the concrete (Sun *et al*. 1999, Hanjari *et al*. 2011). Although the mechanism of frost damage is not completely clear, the water pressure theory proposed by Powers (1945) is supported as a basic idea (Powers 1945). This theory states that, in a low temperature environment, the movement of unfrozen water due to the pressure from frozen water is affected by distance between air voids in concrete, and by shortening the distance between air voids, water movement pressure can be eased and thereby suppressing damage due to expansion. In other words, to suppress deterioration due to frost damage, it is important to entrain good quality air and shorten the distance between air voids (Wong *et al*. 2011).

In Japan, the standard air content prescribed at the time of unloading of ordinary concrete is 4.5%, with a tolerance of ±1.5% (JASS 5 2018, JIS A 5308 2019). In addition, national standards of South Korea (KS F 4009 2016), China (JGJ 55 2011), the United States (ACI 211 2009, ASTM C 94 2020) and Europe (EN 206 2013) also require that a certain amount of air be secured when there is a risk of frost damage. In recent years, in some areas of Japan, where frost damage is common, countermeasures have been established according to the classification of frost damage. For instance, the target air volume at the time of unloading of ready mixed concrete is 5% in severe freezing and thawing damage environment, and 6% in extremely severe freezing and thawing damage environment (MLIT 2017). Entraining 6% of air content is difficult to control, and if the air content becomes excessive, it may lead to a decrease in the strength of the concrete. Moreover, even if the target air volume is secured during concrete production, the air volume may decrease during transportation, pumping, and vibration compaction and it may not be possible to secure the desired air volume in the hardening material. Pumping has been shown to reduce entrained air in the small diameter range of 200μ or less, which is said to contribute to frost damage resistance, and as a result, decrease in scaling resistance has been confirmed (Oyamada *et al*. 2022).

Phase change materials have been studied for their performance in mitigating freeze-thaw damage in concrete (Pilehvar *et al*. 2019, Nayak *et al*. 2019, Li *et al*. 2019, Farnam *et al*. 2017, Tian *et al*. 2022, Yeon and Kim 2018, Bentz and Turpin 2007). Honda *et al*. (2021) investigated the use of a waterproofing agent mainly composed of solid paraffin and an aqueous solution of calcium nitrite and confirmed that solid paraffin has excellent freeze-thaw resistance (Honda *et al*. 2021). Paraffin is a hydrophobic compound, and previous studies have suggested that the addition of hydrophobic compounds improves the frost resistance of concrete (Muzenski *et al*. 2015, Kishimoto *et al*. 2018). Nishi and Nawa (2014a, b) attempted to investigate the mechanism by which hydrophobic

*Corresponding author, Ph.D., Assistant Professor,
E-mail: drunarkat@gmail.com
[a] Ph.D. Student
[b] Assistant Professor
[c] Professor

http://www.techno-press.org/?journal=acc&subpage=7
ISSN: 2287-5301 (Print), 2287-531X (Online)

compounds suppress frost damage deterioration, but the mechanism is currently unknown and further investigation is required (Nishi and Nawa 2014a, b).

Furthermore, in recent years, due to the spraying of anti-freezing agents aimed at preventing the road from freezing in winter, or in marine conditions in cold regions, the combined deterioration of salt damage and frost damage has become a serious problem adversely affecting the mechanical and durability performance (Farnam *et al*. 2015, Qiao *et al*. 2018, Sun *et al*. 2002, Zhou *et al*. 2022, Wang *et al*. 2021, 2022). At present, there is little knowledge about the effect of paraffin on such composite deterioration.

In this study, we investigated the influence of paraffin on the basic physical properties and freeze-thaw resistance of concrete. In terms of basic physical properties, fresh properties and curing properties such as compressive strength were investigated. Regarding freeze-thaw resistance, not only resistance to frost damage but also resistance to combined deterioration with salt damage was investigated. In addition, we clarified the mechanism by which the paraffin mixture improves resistance to frost damage.

2. Experimental

2.1 Materials used and mix-proportion

Table 1 shows the mix proportion of concrete. Paraffin having an average particle size of 0.5 μm was used in the form of an emulsion with a solid content of 30% by mixing with water. The water to cement ratio of concrete was 55% (hereinafter expressed as "W/C"). The target slump was 12 ± 2.5 cm, the target air volume was 5.0 ± 1.0% for concrete containing air entraining agent ("AEC"), and 3.0 ± 1.0% for concrete without air entraining agent ("NonAEC"). These target values were achieved by adjusting the amount of water reducing agent, an AE agent, and an antifoaming agent. Concrete mixed with paraffin was labelled as PC followed by amount of paraffin added.

Table 1 Mix proportions of concretes

Specimen	W/C	Materials (kg/m^3)				Admixture (kg/m^3)			
	(%)	W	C	S	G	PE	Ad	AE	DF
AEC	55	167	304	871	935	-	3.04	0.122	-
NonAEC				874	929	-	4.56	-	0.030
PC 4.5						4.5	5.17	-	0.046
PC 9.0						9	5.17	-	0.060

*W: Tap water, C: Ordinary Portland cement (Specific gravity = 3.16), S: Fine aggregate (Specific gravity = 2.57), G: Coarse aggregate (Specific gravity = 2.65), PE: Paraffin emulsion (Specific gravity = 0.98), Ad: Water reducing agent (mixture of lignosulfonic acid compound and polycarboxylic acid ether),
AE: Air Entraining agent (modified rosin surfactant),
DF: Antifoaming agent (polyalkylene glycol derivative)

2.2 Test methods

2.1 Fresh concrete

In this test, we investigated the effect of paraffin incorporation on fresh properties of concrete. Slump and air content were measured according to JIS A 1101 (2020) and JIS A 1128 (2020).

2.2.2 Bleeding test

The amount of bleeding water when paraffin was incorporated in the concrete was investigated. Bleeding was performed using a container with an inner diameter of 250 mm and an inner height of 285 mm according to JIS A 1123 (2022).

2.2.3 Compressive strength

Generally, certain amount of entrained air is prescribed for concrete subjected to frost damage. Entraining air is found to reduce the compressive strength. But, when paraffin is mixed, the specified amount of air is not entrained, hence it is expected that the strength reduction is suppressed. Therefore, we investigated the compressive strength development when paraffin is mixed. Compressive strength was measured in accordance with JIS A 1108 (2018) using specimens of φ100×200 mm that were cured in water until the age of 28 days. Average of three specimens was taken.

2.2.4 Freeze-thaw test

In this test, the effect of paraffin incorporation on resistance to frost damage alone and also the combined deterioration resistance to frost damage and salt damage was investigated. Freeze-thaw tests were conducted using 100×100×400 mm specimens and performing relative dynamic modulus of elasticity according to JIS A 1148 (2010), Method A. Two freezing mediums: tap water and 3% calcium chloride aqueous solution were used in the experiment. An average of two samples was collected in each test. When 3% $CaCl_2$ aqueous solution was used as the freezing medium, the chloride ion permeability was evaluated by EPMA after 300 freeze-thaw cycles.

2.2.5 Observation of cracks after freeze-thaw test

The purpose of this test was to understand the occurrence of cracks after due to combined deterioration by frost damage and salt damage. The test method proposed by Saichi *et al*. (2002) was used as a reference to observe cracks in the specimen after the freeze-thaw test was completed using a 3% $CaCl_2$ aqueous solution as the freezing medium (Saichi *et al*. 2002). A 100×100×20 mm specimen was cut from the specimen and impregnated with fluorescent resin. After that, using an electron microscope, 200 images were taken from one sample at a magnification of 30 times while illuminating it with black light. Three straight lines (traverse lines) were drawn on each photographed image, and the points where the traverse lines and cracks intersected were counted. The intersection point density was measured using Eq. (1). For reference, we also observed cracks in specimens that were not subjected to freezing and thawing.

$$A = \frac{N}{L} \quad (1)$$

Here, A: point density (points/mm)
N: number of points where the traverse line intersects the crack (piece)
L: total length of traverse line (mm)

2.2.6 Heat generation due to phase change

The mechanism of improvement in freeze-thaw resistance was thought to be due to the paraffin shrinking as the temperature decreased, thereby providing space. Therefore, in this test, we investigated the volume change of paraffin due to temperature change. The temperature change during the freeze-thaw cycle was monitored. In the test, using the mortar composition (W/C = 50%, S/C = 3.0) specified in JIS R 5201 (2015), a φ50×100 mm specimen was prepared and demolded after one day, and cured at 20°C and 60% RH until the age of 7 days. A thermocouple was placed in the center of the specimen and the minimum temperature was -20°C and the maximum temperature was 20°C. The freezing rate was -2.5°C/hr. and the melting rate was 5.0°C/hr. The temperature was kept at -20°C for 4 hours and at 20°C for 4 hours to make a total of 24 hours per cycle.

2.2.7 Frozen water amount

There is a correlation between freeze-thaw resistance and frozen water volume. Therefore, in this test, the amount of frozen water when paraffin was mixed was measured. The amount of frozen water was measured by referring to the test method proposed by Hasegawa *et al.* (2006), focusing on the latent heat during the freezing and thawing of the dry specimen and the saturated specimen (Hasegawa *et al.* 2006). A cement paste specimen with W/C = 50% was prepared in a φ50×100 mm mold with a power-saving couple placed at the center. The amount of paraffin mixed was set at three levels, equivalent to 4.5, 9.0, and 13.5 kg/m^3. After curing in water, it was completely sealed with polyethylene film and plastic wrap film and tested. For a standard, specimens were prepared by pre-curing W/C = 30% cement paste specimen in water for 7 days and then drying for 28 days in an environment with a relative humidity of 30% or less. Based on the method of measuring the amount of frozen water and the accumulated latent heat temperature detected from the temperature difference between the saturated cement paste specimen and the dry specimen due to freezing and thawing, the amount of frozen water in the cement hardened body was calculated. The freeze-thaw cycle was set for a minimum temperature of -30°C and maximum temperature of 10°C. The freezing rate was -2.5°C/hr. and the melting rate was 5.0°C/hr. The temperature was kept at -30°C for 2 hours and at 10°C for 3 hours to make a total of 29 hours per cycle.

2.2.8 Air void spacing

The cell spacing coefficient was measured in order to investigate the mechanism of improvement in freeze-thaw resistance when paraffin is mixed. The air void spacing factor was determined by the linear traverse method according to ASTM C457 (2006). A 90×90×20 mm specimen was cut from the center of a φ100×200 mm specimen that had been cured in water until the age of 28 days.

2.2.9 Observation of the state of paraffin

This test was conducted to confirm the dispersion status of paraffin in hardened matrix. In observing the state of paraffin dispersion, a cement paste containing 50% water-cement ratio and 3% paraffin emulsion to cement ratio was molded into a diameter of φ20×3 mm. Samples sealed and cured until 28 days old were measured with a micro-Raman spectrophotometer. In the preliminary test, the paraffin emulsion and the cement paste were individually measured, and it was confirmed that the Raman shift of paraffin appeared around 2900 cm^{-1}. A color image was created based on the specific peak. For example, large peaks were assigned to reddish range and smaller peaks towards blue.

3. Results and discussion

3.1 Properties of fresh concrete

The slump was 16.5 cm for AEC, 16.0 cm for Non-AEC, 15.0 cm for PC4.5, and 13.0 cm for PC9.0. Air content was 5.4% for AEC, 2.2% for NonAEC, 2.9% for PC4.5, and 3.2% for PC9.0. The slump decreased slightly with the addition of paraffin. This is because the paraffin emulsion was mixed within the unit water volume. The air content was within the target value of 3.0±1.0% for NonAEC and 5.0±1.0% for AEC. The addition of paraffin decreased the bleeding as shown in Fig. 1. The amount of bleeding of paraffin added PC 4.5 and PC 9.0 was approximately 30% lesser than that of NonAEC. This effect tended to increase as the amount of paraffin added increased. This is considered to be because the viscosity of the concrete was increased by mixing the paraffin emulsion.

3.2 Compressive strength

The 28-day compressive strength is shown in Fig. 2. The compressive strength of PC 4.5 and PC 9.0 was found to be comparable to that of NonAEC. On the other hand, the compressive strength of AEC, was about 20% lower than that of NonAEC. Addition of paraffin did not reduce the compressive strength as seen in air entrained concrete.

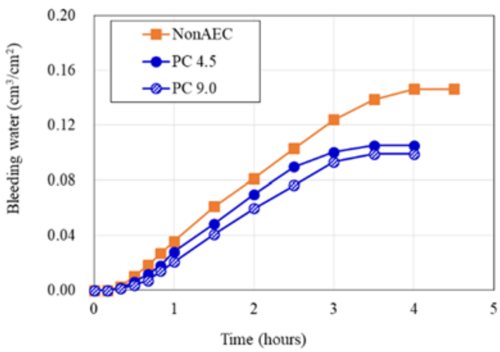

Fig. 1 Bleeding amount

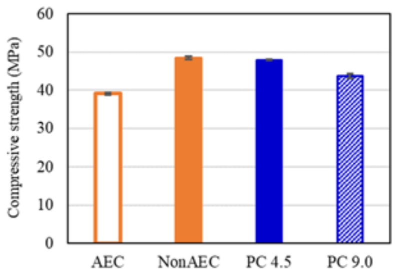

Fig. 2 Compressive strength

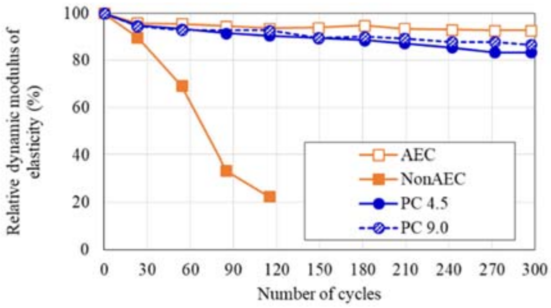

Fig. 3 Freeze-thaw test using tap water

3.3 Freeze-thaw resistance

To examine the resistance of concrete with paraffin against freezing and thawing, the change in relative modulus of elasticity was used as one of the indicators.

Fig. 3 shows the relative dynamic modulus of elasticity when tap water is used as the freezing medium, and Fig. 4 shows the mass change rate. The RDME of AEC did not decrease even after 300 cycles. On the other hand, NonAEC began to decrease immediately after the start of freezing and thawing and fell below 60% at the 90th cycle. The RDME of PC 4.5 and PC 9.0 did not decrease up to 300 cycles and maintained more than 80%, like AEC. No clear difference was observed in the respective mass reductions when tap water was used. Nishi and Nawa (2014a) reported that the introduction of a hydrophobic compound-based shrinkage reducing agent into concrete suppresses the movement of unfrozen water or the penetration of ice crystals, thereby lowering the expansion pressure and improving frost damage resistance (Nishi and Nawa (2014a). Which indicates that the paraffin used in this study, being hydrophobic, also exhibited similar expansion resistance.

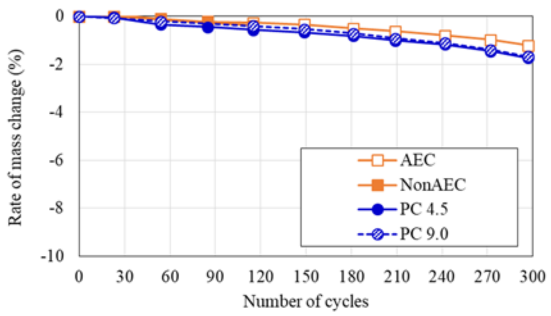

Fig. 4 The rate of mass change using tap water

3.4 Composite deterioration under a combination of freeze-thaw and salt environment

3.4.1 Change in relative dynamic modulus of elasticity

The RDME of the specimens subjected to composite deterioration condition, in which 3% $CaCl_2$ aqueous solution is used as the freezing medium was determined and the results are shown Fig. 5 and their respective mass change rate are show in Fig. 6. NonAEC dropped to less than 60% after 120 cycles. The reason why the RDME reduction was lower when using a 3% $CaCl_2$ aqueous solution compared to when tap water was used is thought to be due to the increased strength influenced by chloride ions. PC 4.5 and PC 9.0 were about 80% at 300 cycles, like AEC. There was no significant difference in the RDME between tap water and 3% $CaCl_2$ aqueous solution. The mass change rate when using 3% $CaCl_2$ aqueous solution was different from that when using tap water, and a clear mass decrease was confirmed as the freeze-thaw cycle progressed immediately after the start of the test.

The mass change rate of NonAEC was about -12% at 120 cycles, confirming severe scaling. On the other hand, the mass change rates of PC 4.5 and PC 9.0 were larger than those of AEC, but were about 5.0% and 4.5%, respectively, at 120 cycles, indicating reduced scaling. This suggests that the addition of paraffin can suppress frost damage in an environment supplied with chloride ions. These factors were further justified by investigations in the following sections.

3.4.2 Chloride ion penetration

Since the relative dynamic modulus of elasticity of the paraffin mixed concrete did not decrease much, a chloride

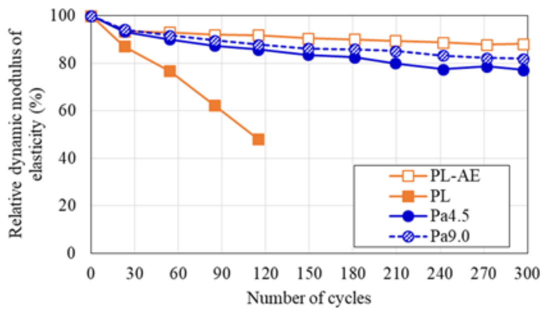

Fig. 5 Freeze-thaw test using 3% $CaCl_2$

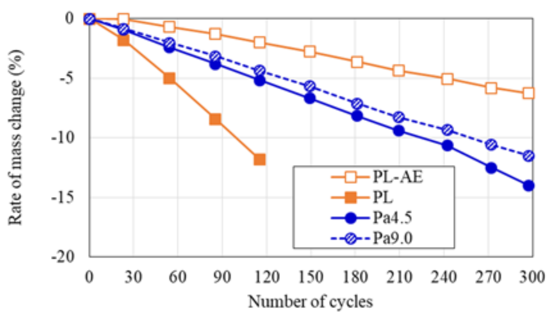

Fig. 6 The rate of mass change in 3% $CaCl_2$

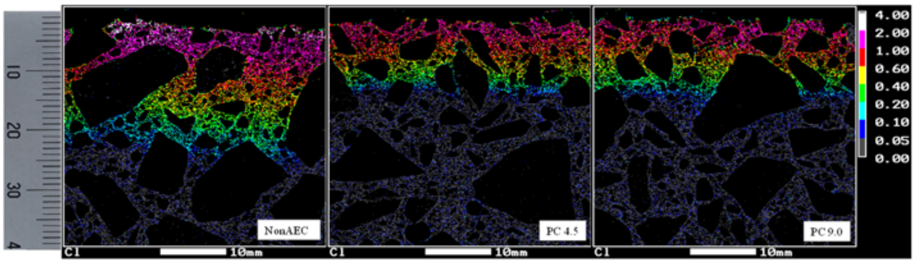

Fig. 7 Chloride ion penetration after combined deterioration test

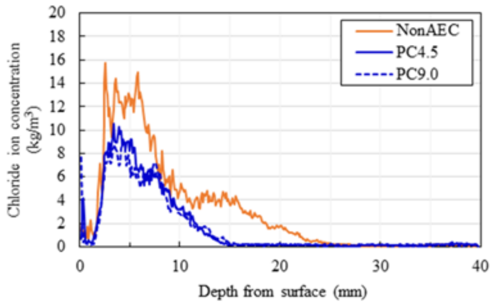

Fig. 8 Distribution of chloride ion concentration

profile was also analyzed for each concrete. Fig. 7 shows the permeation of chloride ions observed by EPMA using the specimen after freezing and thawing. Fig. 8 shows the chloride ion concentration distribution at each depth from the surface. In addition, since the RDME of NonAEC fell below 60% after 120 cycles of the freeze-thaw test, other samples were not subjected to the freeze-thaw action until they reached 300 cycles. It shows the permeation of chloride ions after being immersed in a 3% $CaCl_2$ aqueous solution. In the NonAEC, the penetration depth of chloride ions reached about 25 mm, and the chloride ion concentration in the surface layer was about 50 kg/m^3. On the other hand, for PC 4.5 and PC 9.0, it was about 15 mm, and 25 kg/m^3 respectively, which is lower than NonAEC. From this, it was confirmed that when paraffin was added, chloride ion permeation was suppressed in a composite deterioration environment of freeze-thaw and salt compared to when paraffin was not mixed.

3.4.3 Internal crack observation

To substantiate the resistance of paraffin mixed concrete exhibited in the results of dynamic modulus and chloride penetration, the internal cracks were observed. The Fig. 9 shows images of cracks observed after freezing and thawing. Cracking of NonAEC tended to occur most often at the interface between aggregate and cement paste. In addition, many cracks in the cement paste and inside the aggregate were also observed. For PC 4.5 and PC 9.0, cracks occurred at the interface between the aggregate and cement paste, but were less frequent than NonAEC, and almost no cracks occurred in the cement paste. Adding to this, bleeding amount shown in Fig. 1, tended to decrease for paraffin mixed concrete. One reason for the decrease in cracking at the aggregate interface is the decrease in the transition zone at the aggregate interface. The point density of the cracks of the test piece before freezing and thawing was 0.008 points/mm for NonAEC, 0.009 points/mm for PC4.5, and 0.006 points/mm for PC9.0. On the other hand, the point density of cracks after freezing and thawing was 0.193 points/mm for NonAEC, 0.046 points/mm for PC4.5, and 0.028 points/mm for PC9.0.

The point densities for PC 4.5 and PC 9.0 after the freeze-thaw test were 24% and 12% lower than NonAEC, respectively. From this, in the composite deterioration test, the reason why chloride ions permeated NonAEC more than paraffin added concrete was that more cracks were generated inside due to the action of freezing and thawing.

3.5 Mechanism of improvement of freeze-thaw resistance

Farnam *et al*. (2016) reported that paraffin oil can lower the freezing temperature by generating latent heat when the phase changes from liquid to solid as the temperature decreases (Farnam *et al*. 2016). It shows that it is promising as a concrete pavement material that melts ice and snow. Therefore, the latent heat of paraffin was also investigated in this study. Fig. 10 shows the temperature history during freezing. In the case of water, the effect of latent heat was confirmed around -6°C. Conversely, paraffin alone is solid at 20°C, hence phase change did not occur, and the effect of latent heat was not confirmed. In the case of paraffin emulsion with a concentration of 30%, the effect of latent heat was confirmed at around -6°C, like water. Since 70% of the paraffin emulsion is water, and latent heat was generated by the phase change of water. So, the freeze-thaw

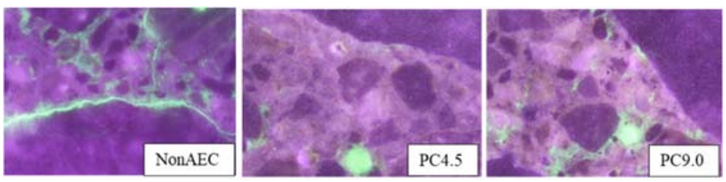

Fig. 9 Observed cracks after freeze-thaw test

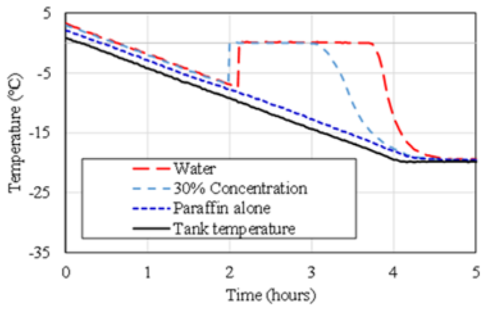

Fig. 10 Temperature history

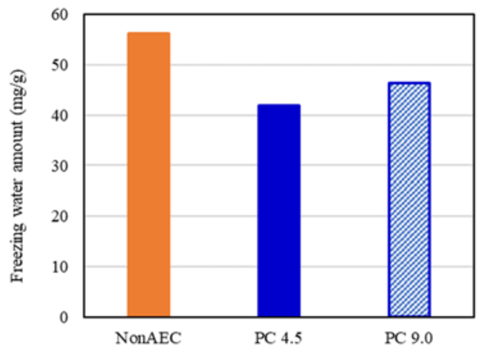

Fig. 11 Frozen water amount

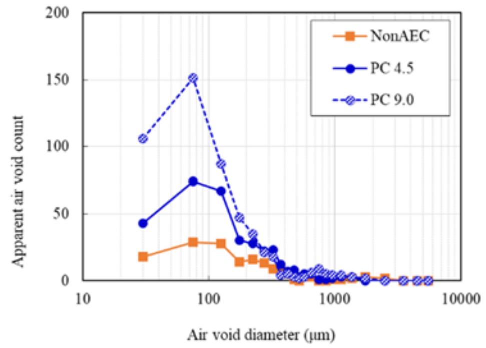

Fig. 12 Apparent air void content

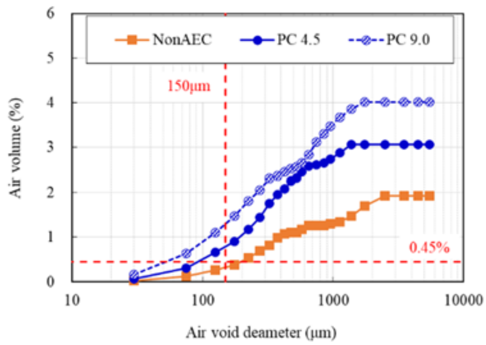

Fig. 13 Air void volume versus void diameter

resistance when mixed with paraffin was not affected by latent heat of paraffin alone. Fig. 11 shows the amount of frozen water. The amount of frozen water in PC4.5 and PC9.0 when paraffin was used was less than that of NonAEC. From this, it is considered that one of the reasons for the improvement in freeze-thaw resistance when paraffin was added was that the amount of frozen water decreased due to the addition of paraffin.

The air void spacing factors were 509 μm for NonAEC, 305 μm for PC4.5, and 232 μm for PC9.0. It was confirmed that the air void spacing factor tended to decrease as the amount of paraffin added increased. Especially, for PC 9.0, it was under 250 μm, which is said to have high freeze-thaw resistance.

Fig. 12 shows the number of air voids for each void diameter. The number of air voids is expressed as the apparent number of voids, because paraffin was also accounted for. Fig. 13 shows the air content at each pore size in the hardened material. A study by Sakata *et al.* (2012) showed that the more the 150 μm air voids, the higher the frost damage resistance, and it was reported that it was necessary to contain 0.45% or more of such pores in the hardening material (Sakata *et al.* 2012). When paraffin was added, fine air voids of 250 μm or less tended to increase. Regarding the air content in the hardened specimen, the air content of PC 4.5 and PC 9.0 was larger than that of NonAEC. At the time of checking the fresh properties, the difference in air content in NonAEC between Pa4.5 and Pa9.0 were 0.7% and 1.0%, but were large, 1.1% and 2.1%, in the hardened specimen. In addition, the amount of air void with a diameter of 150 μm or less was 0.27% for NonAEC, 0.67% for PC 4.5 and 1.10% for PC 9.0. Therefore, the amount of pores was larger than the required pore amount of 0.45% for high freeze-thaw resistance.

From the above, the increase in freeze-thaw resistance when paraffin was added is due to the increase in the amount of air voids in the specific air void diameter, which is believed to contribute to freeze-thaw resistance.

Fig. 14 shows images from Raman spectroscopy. It shows that paraffin with a size of 200 μm or less was evenly distributed in the cement paste. Considering that the paraffin particles in the emulsion were about 0.5 μm in size, it is presumed that they exist as aggregates in the cement paste. From this, it is considered that the apparent number of air voids increased in Fig. 12 was due to the distribution of aggregates of paraffin particles in the concrete.

From the above, the improvement of freeze-thaw resistance when paraffin is mixed is due to the fact that paraffin particles form aggregates of a predetermined size and exist in concrete, acting as substitutes for air voids and increasing the apparent intercellular spacing coefficient. Therefore, the pressure during the freeze-thaw cycle was relieved.

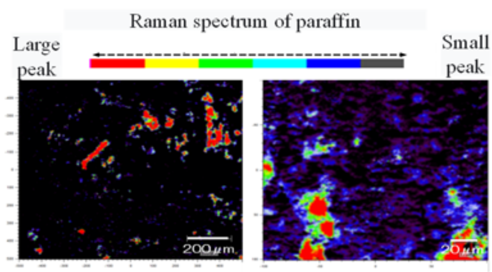

Fig. 14 Raman spectroscopy imaging diagram

4. Conclusions

In this study, we conducted an investigation to clarify the combined deterioration resistance of freeze-thaw and salt when paraffin was mixed. Specifically, we investigated basic physical properties, freeze-thaw resistance, and freeze-thaw resistance in an environment where chloride ions were supplied to concrete mixed with paraffin. The findings obtained are shown below.

- The amount of bleeding water paraffin mixed concrete PC 4.5 and PC 9.0 was approximately 30% lesser than that of NonAEC.
- The compressive strength was about the same as that of concrete without paraffin. By adding paraffin, the problem of strength reduction in air entrained concrete can be solved.
- By incorporating paraffin, the decrease in the relative dynamic elastic modulus was suppressed without entraining air, and the relative dynamic elastic modulus was maintained at 80% or more after 300 freeze-thaw cycles.
- Even when freezing and thawing was performed in an environment where chloride ions were supplied, the freeze-thaw resistance effect of incorporating paraffin was confirmed, and it was observed that the mass change rate due to scaling was suppressed by more than twice.
- Under a composite deterioration condition of freeze-thaw and salt, the occurrence of internal cracks was controlled, leading to reduced permeation of chloride ions.
- The amount of frozen water is reduced, and the mixed paraffin particles were present in the concrete as pore fillers with a size of 200 μm or less. By this, the apparent air void spacing factor was lowered, and the pressure was relieved.

Conflict of interest

There are no known conflicts of interest associated with this publication.

Funding

This research did not receive any specific grant from funding agencies in the public, commercial, or not-for-profit sectors.

References

ACI 211 (2009), American Concrete Institute, Standard practice for selecting proportions for normal, heavyweight, and mass concrete: State of Michigan, USA.

ASTM C 457 (2006), America Society for Testing and Materials, Standard Test Method for Microscopical Determination of Parameters of the Air-Void System in Hardened Concrete: ANSI.

ASTM C 94 (2020), ASTM International, Standard specification for ready-mixes concrete, American National Standards Institute: Commonwealth of Pennsylvania, USA.

Bentz, D.P. and Turpin, R. (2007), "Potential applications of phase change materials in concrete technology", *Cem. Concr. Res.*, **29**, 527-532. https://doi.org/10.1016/j.cemconcomp.2007.04.007

EN 206 (2013), European Standard, Concrete. Specification, performance, production and conformity, European Committee for Standardization: European Union.

Farnam, Y., Wiese, A., Bentz, D., Davis, J. and Weiss, J. (2015), "Damage development in cementitious materials exposed to magnesium chloride deicing salt", *Constr. Build. Mater.*, **93**, 384-392. https://doi.org/10.1016/j.conbuildmat.2015.06.004

Farnam, Y., Krafcik, M., Liston, L., Washington, R., Erk, K., Tao, B. and Weiss, J. (2016), "Evaluating the Use of Phase Change Materials in Concrete Pavement to Melt Ice and Snow", *J. Mater. Civ. Eng.*, **28**(4). https://doi.org/10.1061/(ASCE)MT.1943-5533.0001439

Farnam, Y., Esmaeeli, H.S., Zavattieri, P.D., Haddock, J. and Weiss, J. (2017), "Incorporating phase change materials in concrete pavement to melt snow and ice", *Cem. Concr. Res.*, **84**, 134-145. https://doi.org/10.1016/j.cemconcomp.2017.09.002

Hanjari, K.Z., Utgenannt, P. and Lundgren, K. (2011), "Experimental study of the material and bond properties of frost-damaged concrete", *Cem. Concr. Res.*, **41**, 244-254. https://doi.org/10.1016/j.cemconres.2010.11.007

Hasegawa, S., Mitsuishi, N., Akahori, Y. and Nawa, T. (2006), "A Proposal of a Method for Measuring the Frozen Water Volume of Water in Cured Cement", *Proc. Jpn. Concr. Inst.*, **28**(1), 851-856. [In Japanese] https://data.jci-net.or.jp/data_pdf/28/028-01-1139.pdf

Honda, D., Quy, N.X., Kim, J. and Hama, Y. (2021), "Influence of drying on frost resistance of mortar using a nitrite corrosion inhibitor and paraffin waterproofing agent", *Constr. Build. Mater.*, **283**, 1-16. https://doi.org/10.1016/j.conbuildmat.2021.122581

JASS 5 (2018), Japanese Architectural Standard Specification, Japanese Architectural Standard Specification Reinforced Concrete Work: Japan.

JGJ 55 (2011), Chinese National Standard, Specification for mix proportion design of ordinary concrete: China.

JIS A 1101 (2020), Japanese Industrial Standards, Method to test for slump to concrete, Japanese Standards Association: Tokyo, Japan.

JIS A 1108 (2018), Japanese Industrial Standards, Method to test for compressive strength of concrete, Japanese Standards Association: Tokyo, Japan

JIS A 1123 (2022), Japanese Industrial Standards, Method to test for bleeding of concrete, Japanese Standards Association: Tokyo, Japan.

JIS A 1128 (2020), Japanese Industrial Standards, Method to test for air content of fresh concrete by pressure method, Japanese Standards Association: Tokyo, Japan.

JIS A 1148 (2010), Japanese Industrial Standards, Method to test for resistance of concrete to freezing and thawing, Japanese Standards Association: Tokyo, Japan.

JIS A 5308 (2019), Japanese Industrial Standards, Ready-mixed concrete, Japanese Standards Association: Tokyo, Japan.

JIS R 5201 (2015), Japanese Industrial Standards, Physical test methods for cement, Japanese Standards Association: Tokyo, Japan.

KS F 4009 (2016), Korean Industrial Standards, Ready-mixed concrete, Korean Standards Association: Seoul, Korea.

Kishimoto, G., Kim, J., Choi, H. and Hama, Y. (2018), "Influence of silicone oil on durability of portland blast furnace slag cement mortar", *J. Adv. Concr. Technol.*, **16**, 110-123. https://doi.org/10.3151/jact.16.110

Li, W., Ling, C., Jiang, Z. and Yu, Q. (2019), "Evaluation of the potential use of form-stable phase change materials to improve the freeze-thaw resistance of concrete", *Constr. Build. Mater.*, **203**, 621-632. https://doi.org/10.1016/j.conbuildmat.2019.01.098

MLIT (2017), Ministry of Land, Infrastructure, Transport and Tourism, Reference materials on measures against freezing and thawing resistance in the Tohoku region (draft). [In Japanese]

Muzenski, S., Flores-Vivian, I. and Sobolev, K. (2015), "Durability of superhydrophobic engineered cementitious composites", *Constr. Build. Mater.*, **81**, 291-297. https://doi.org/10.1016/j.conbuildmat.2015.02.014

Nayak, S., Lyngdoh, G.A. and Das, S. (2019), "Influence of microencapsulated phase change materials (PCMs) on the chloride ion diffusivity of concretes exposed to Freeze-thaw cycles: Insights from multiscale numerical", *Constr. Build. Mater.*, **212**, 317-328. https://doi.org/10.1016/j.conbuildmat.2019.04.003

Nishi, H. and Nawa, T. (2014a), "Property of the hydrophobic compound based drying shrinkage reducing agent which improved deterioration resistance by frost action", *Trans. AIJ. J. Struct. Constr. Eng.*, **79**(696), 191-200. [In Japanese] https://doi.org/10.3130/aijs.79.191

Nishi, H. and Nawa, T. (2014b), "Study on frost damage degradation in hydrated cement using hydrophobic compound", *Trans. AIJ. J. Struct. Constr. Eng.*, **79**(696), 1415-1424. [In Japanese] https://doi.org/10.3130/aijs.79.1415

Oyamada, T., Misosaku, T., Tkahasi, K. and Shiina, T. (2022), "Effects of Various Construction Processes on the Tunnel Lining Concrete Air and Its Frost Resistance", *Proc. Jpn. Concr. Inst.*, **44**(1), 526-531. [In Japanese]

Pilehvar, S., Szczotok, A.M., Rodríguez, J.F., Valentini, L., Lanzón M., Pamies, R. and Kjøniksen, A.L. (2019), "Effect of freeze-thaw cycles on the mechanical behavior of geopolymer concrete and Portland cement concrete containing micro-encapsulated phase change materials", *Constr. Build. Mater.*, **200**, 94-103. https://doi.org/10.1016/j.conbuildmat.2018.12.057

Powers, T.C. (1945), "A Working Hypothesis for Further Studies of Frost Resistance of Concrete", *J. Am. Concr. Inst.*, 16(4), 245-272. https://www.concrete.org/publications/internationalconcreteabstractsportal/m/details/id/8684

Qiao, C., Suraneni, P. and Weiss, J. (2018), "Damage in cement pastes exposed to NaCl solutions", *Constr. Build. Mater.*, **171**, 120-127. https://doi.org/10.1016/j.conbuildmat.2018.03.123

Saichi, M., Shinohe, H. and Mihashi, H. (2002), "Quantification of internal cracks developed within frost-damaged concrete", *Concr. Res. Technol.*, **13**(1), 13-24. [In Japanese] https://doi.org/10.3151/crt1990.13.1_13

Sakata, N., Sugamata, T., Hayashi, D. and Hashimoto, M. (2012), "Investigation for relationship between frost damage resistance and air-void system in concrete", *Concr. Res. Technol.*, **23**(1), 35-47. [In Japanese] https://doi.org/10.3151/crt.23.35

Sun, W., Zhang, Y.M., Yan, H.D. and Mu, R. (1999), "Damage and damage resistance of high strength concrete under the action of load and freeze-thaw cycles", *Cem. Concr. Res.*, **29**, 1519-1523. https://doi.org/10.1016/S0008-8846(99)00097-6

Sun, W., Mu, R., Luo, X. and Miao, C. (2002), "Effect of chloride salt, freeze-thaw cycling and externally applied on the performance of the concrete", *Cem. Concr. Res.*, **32**, 1859-1864. https://doi.org/10.1016/S0008-8846(02)00769-X

Tian, Y., Lai, Y., Pei, W., Qin, Z. and Li, H. (2022), "Study on the physical mechanical properties and freeze-thaw resistance of artificial phase change aggregates", *Constr. Build. Mater.*, **329**, 127-225. https://doi.org/10.1016/j.conbuildmat.2022.127225

Wang, Y., Li, J., Ueda, T., Zhang, D. and Deng, J. (2021), "Meso-scale mechanical deterioration of mortar subjected to freeze thaw cycles and sodium chloride attack", *Cem. Concr. Compos.*, 117. https://doi.org/10.1016/j.cemconcomp.2020.103906

Wang, Y., Liu, Z., Zhang, B. and Fu, K. (2022), "A time-dependent diffusive model for the simulation of chloride penetration in concrete considering the effect of natural salt freeze-thaw cycles", *Cold Regions Sci. Technol.*, **201**. https://doi.org/10.1016/j.coldregions.2022.103622

Wong, H.S., Pappas, A.M., Zimmerman, R.W. and Buenfeld, N.R. (2011), "Effect of entrained air voids on the microstructure and mass transport properties of concrete", *Cem. Concr. Res.*, **41**, 1067-1077. https://doi.org/10.1016/j.cemconres.2011.06.013

Yeon, J.H. and Kim, K.K. (2018), "Potential applications of phase change materials to mitigate freeze-thaw deteriorations in concrete pavement", *Constr. Build. Mater.*, **117**, 202-209. https://doi.org/10.1016/j.conbuildmat.2018.05.113

Zhou, J., Wang, G., Liu, P., Guo, X. and Xu, J. (2022), "Concrete Durability after Load Damage and Salt Freeze–Thaw Cycles", *Mater.*, **15**(13), 4380. https://doi.org/10.3390/ma15134380

CC